Chromatin Condensation Is Confined to the Loop and Involves an All-or-None Structural Change

Cecilia Balbi,* Paola Sanna,* Paola Barboro,* Ingles Alberti,* Marta Barbesino,*# and Eligio Patrone#
*Istituto Nazionale per la Ricerca sul Cancro, 16132 Genoa, and #Istituto di Studi Chimico-Fisici di Macromolecole Sintetiche e Naturali, 16146 Genoa, Italy

ABSTRACT Using differential scanning calorimetry in combination with pulsed field gel electrophoresis, we relate here the changes in the thermal profile of rat liver nuclei induced by very mild digestion of chromatin by endogenous nuclease with the chain length distribution of the DNA fragments. The enthalpy of the endotherm at 106°C, which reflects the denaturation of the heterochromatic domains, decreases dramatically after the induction of a very small number of double-strand breaks per chromosome; the thermal transition disappears when the loops have undergone on average one DNA chain scission event. Quantitative analysis of the experimental data shows that the loop behaves like a topologically isolated domain. Also discussed is the process of heterochromatin formation, which occurs according to an all-or-none mechanism. In the presence of spermine, a strong condensation agent, only the loops that have undergone one break are able to refold, in confirmation of the extremely cooperative nature of the transition. Furthermore, our results suggest a relationship between the states that give rise to the endotherms at 90°C and 106°C and the morphologies referred to as class II and class III in a previous physicochemical study of the folding of chromatin fragments (Widom, 1986. *J. Mol. Biol.* 190:411–424) and support the view that the overall process of condensation follows a sequential (two-step) pathway.

INTRODUCTION

In a recent review Felsenfeld (1996) has rethought within a thermodynamic framework the molecular mechanisms involved in the process of activation of eukaryotic genes. The binding of transcription factors must overcome the free energy of interaction of histones with DNA, but additional barriers can also arise, at the supranucleosomal level, from the folding of chromatin into higher-order structures; those genes that are permanently turned off during cell differentiation are expected to be packaged in more stable structural domains compared with the competent ones (van Holde, 1989) to oppose undesired reactivation. Besides the high stability of heterochromatin, the mechanism of the conformational change between the unfolded and condensed states (assumed to be an all-or-none process) could also play a functional role during development, converting a slowly changing concentration of transcription factors into a sharp transition between different cellular populations.

In a previous work on the thermodynamics of H1-induced chromatin folding (Russo et al., 1995), we basically referred to the same model for gene silencing commented on in Felsenfeld's article, to strengthen the biological relevance of investigations on the physical chemistry of heterochromatin formation. It must be pointed out, however, that for this approach to be useful the structural situation existing inside the nucleus should be preserved as far as possible in the experiments in vitro. Even if one relies on the major outcomes of physical observations on chromatin fragments, it should be taken into account that key architectural features of the genome are lost during the extraction of the material. Early in the digestion with nucleases the polynucleosomal chain is released from the constraints arising from the organization into topologically isolated loops, which might represent a major device for heterochromatic condensation. In a classical investigation on the cation-induced folding of long chromatin fragments, Widom (1986) noted that refolded chromatin can be observed in the electron microscope in the form of long rope-like aggregates of 30-nm filaments, resembling the loops of metaphase chromosomes; experiments carried out using different cations over a wide range of concentration showed, however, that aggregation of the filaments invariably precedes the completion of the structural change. The fact that careful refolding experiments yield a material that has not attained the fully ordered state suggests that the closing of the polynucleosomal chain in the loop is required for the regular packaging of nucleosomes in the heterochromatic regions. The application of electron tomography methods to chromatin in situ could be used in principle to image the path of the 30-nm fiber inside the folded domains, but the results obtained on thin nuclear sections indicate that only isolated fibers can be successfully reconstructed by tomographic structural analysis (Woodcock, 1992).

In a series of related papers (Balbi et al., 1989; Cavazza et al., 1991; Barboro et al., 1993; Russo et al., 1995; Allera et al., 1997) we have shown that the conformation of chromatin, both isolated and in situ, represents an almost ideal subject for thermodynamic investigations using simple differential scanning calorimetry (DSC) techniques. The DSC profile of unfolded chromatin essentially reflects the denaturation of the two energetically distinguishable domains,

Received for publication 14 October 1998 and in final form 12 August 1999.

Address reprint requests to Dr. Cecilia Balbi, Istituto Nazionale per la Ricerca sul Cancro, Largo Rosanna Benzi, 10 I-16132 Genoa, Italy. Tel.: 39-10-5600023; Fax: 39-10-5600210; E-mail: balbi@hp380.ist.unige.it.

0006-3495/99/11/2725/11 $2.00

the linker and core particle DNA (Balbi et al., 1989), which occur at 75°C and 90°C, respectively. After chromatin refolding the latter domain gives rise to an additional heat absorption peak at 106°C (Cavazza et al., 1991), which is related to the melting of the DNA of core particles packaged inside condensed (heterochromatic) regions. The capability of DSC to detect changes in the conformation of chromatin has therefore been exploited to develop thermodynamic models of the process of condensation induced by salts (Cavazza et al., 1991; Labarbe et al., 1996) or H1 binding (Russo et al., 1995), as well as to characterize the status of nuclear chromatin during cell transformation (Barboro et al., 1993) and apoptosis (Allera et al., 1997).

A major advance in the application of DSC to the study of fine aspects of the mechanisms of formation of heterochromatin has been attained in this work by refining the structural attribution of the 106°C endotherm (Barboro et al., 1993). Indeed, this heat absorption peak can be deconvolved into two Gaussian components at 100°C and 106°C, showing that interphase chromatin is organized into two levels of folding of different stabilities, the precise nature of which remains to be established (Cavazza et al., 1991; Barboro et al., 1993). The analysis of the structural changes associated with the opening of the loop by mild DNA digestion with endogenous nuclease reported in this paper definitively demonstrates that heterochromatin formation gives rise to the 106°C transition, while isolated or loosely aggregated 30-nm fibers denature at 100°C. Getting back to the problem of the thermodynamic description of the structural changes underlying silencing, our results show for the first time that condensation involves an all-or-none transition as a consequence of the constraints imposed by the loop.

MATERIALS AND METHODS

Preparation and autodigestion of rat liver nuclei

Hepatocytes were isolated from livers of male Fisher F-344 rats (Charles River, Como, Italy), following the procedure reported in a previous paper (Barboro et al., 1996), and nuclei were prepared according to a continuous (in flow) method, as already described (Balbi et al., 1989; Barboro et al., 1996). A dilute (0.5×10^6 cells/ml) suspension of hepatocytes in dissociation medium (DM), consisting of 75 mM NaCl and 24 mM Na_2EDTA (pH 7.8), was mixed at 4°C with an equal volume of DM containing 1% (v/v) Triton X-100 by pumping into a small-volume mixing chamber and conveyed through a Teflon tube 0.1 cm in diameter and 10^2 cm long at a volume rate of flow of 1 ml/min. The high concentration of Na_2EDTA was required to effectively prevent the activation of the Ca^{2+}/Mg^{2+}-dependent endogenous nuclease (Balbi et al., 1989). The buffers were also supplemented with a mixture of protease inhibitors (5 mM $Na_2S_2O_5$, 1 mM phenylmethylsulfonyl fluoride, 0.5 mM benzamidine, 25 μg/ml aprotinin). Nuclei were then recovered by centrifugation at $2500 \times g$, and the nuclear pellet was resuspended in a large excess of digestion buffer. As pointed out by Filipski et al. (1990), the composition of the buffer used in the preparation of nuclei can affect the autodigestion process. We have found that the autodigestion buffer used in a previous work (Barboro et al., 1996) to isolate the nuclear matrix-intermediate filament complex from rat hepatocytes (3 mM $MgCl_2$, 3 mM $CaCl_2$, 10 mM Tris-HCl, pH 7.8) slowly activates the endogenous nuclease when the incubation is carried out at 4°C and is therefore suitable for characterizing the early stages of DNA cleavage. Under these experimental conditions the onset of digestion is detected after an incubation of 30 min, while fragmentation into oligonucleosomes occurs when digestion is allowed to proceed for 18 h. After the required incubation time the nuclei were resuspended in a large excess of DM to stop digestion and pelleted by centrifugation at $10{,}000 \times g$ for DSC determinations or at $2500 \times g$ for embedding in agarose and electron microscopy.

Pulsed field gel electrophoresis and quantitative analysis of the densitometric tracings of the gels

A milligram and a half of nuclear pellet, corresponding to $1–2 \times 10^7$ nuclei, was embedded in agarose plugs; deproteinization of DNA in the plugs by incubation at 37°C for 18 h in 10 mM NaCl, 25 mM Na_2EDTA, 10 mM Tris-HCl (pH 9.5), containing 10% *N*-lauroylsarcosine and 3.3 μg/ml proteinase K (Serva), was carried out exactly as described by Filipski et al. (1990). Pulsed field gel electrophoresis (PFGE) of DNA was carried out on 1.5% agarose gels in a Bio-Rad system, comprising a horizontal gel chamber, a model 220/20 power supply, and a Pulsewave 760 switcher. The samples were run at 10°C for 24 h in TBE buffer (45 mM borate, 1 mM Na_2EDTA, 45 mM Tris-HCl, pH 8) at a voltage gradient of 6 V/cm; the switch time ramped linearly from 5 to 50 s or from 25 to 75 s, depending on the average chain length of the DNA. Yeast chromosomal DNA and λ phage ladder (Bio-Rad) were used as size markers. The gels were stained with 0.5 μg/ml ethidium bromide (EB) and photographed in UV light in an LKB 2011 transilluminator through an orange filter. Because of the high value of the binding constant of EB to DNA, which is equal to $1.3 \times 10^6\ M^{-1}$ for rat liver DNA (Parodi et al., 1975), *r*, the ratio of bound dye to DNA phosphate, assumes, at the above EB concentration, the saturation value (0.17) over a wide range of DNA concentrations; therefore, the densitometric tracings of the gels can be used for the quantitation of DNA as a function of the distance migrated *D*, which in our experiments is in the range 1–8 cm. The negatives were scanned in a Kontron Elektronic Vidas 2.1 image analysis system, and the amount of DNA A_D that migrated between $D + \epsilon$ and $D - \epsilon$ was evaluated by integration of the optical density curve for ~20 values of *D,* with ϵ between 0.1 and 0.2 cm. The distances migrated *D* were converted to *t*, the chain lengths of the DNA fragments and the weight fraction of the latter, determined by the relationship

$$W_t = \frac{A_t}{\sum_t A_t \Delta t} \tag{1}$$

where W_t is the weight fraction of the DNA fragment of chain length *t* and Δt is the chain length increment corresponding to $D_t - \epsilon$ and $D_t + \epsilon$. Because the major object of this study is the relation between internucleosomal DNA cleavage and the stability of heterochromatin, it is convenient to convert the lengths expressed in base pairs, obtained by the comparison of the migration of nuclear DNA with that of the standards, to the number of nucleosomes by dividing their values by 200, the nucleosome repeat length of rat liver chromatin (van Holde, 1989).

Electron microscopy and digital image analysis of thin nuclear sections

Nuclei incubated for different time periods in the digestion buffer were collected by centrifugation as described above, embedded in Poly/Bed 812 Resin (Polysciences), and sectioned as reported in a previous paper (Barboro et al., 1993). After staining with 5% uranyl acetate in 50% ethanol followed by 0.4% aqueous lead citrate, the nuclear sections were photographed at ×44,600 in a Zeiss LEO 900 electron microscope operating at 80 kV.

Images of nuclei were directly acquired from negatives with a CCD camera and digitized in a 512×768 array of pixels, with gray levels varying from 0 (black) to 255 (white); 24–36 randomly selected areas were digitized per digestion time. The analysis was carried out at a fixed

resolution of 2 nm. Image enhancement was performed using a 3 × 3 high-pass filter; this filter reduces the contrast of large, slowly changing components of the image and allows maximum contrast between chromatin and the background to be obtained. The gray levels were then measured along random lines, and $\sim 10^3$ values of the linear transverse length (the length of the intersection of the line with the fiber) were determined interactively. The free path between fibers was measured according to the same procedure, using a different set of processed images. The data were stored in ASCII files for statistical analysis.

Other methods

The histone complement was obtained by acid extraction of nuclei according to the method of Panyim et al. (1971) and run on 15% sodium dodecyl sulfate-polyacrylamide gels (Laemmli, 1970). DSC determinations were performed as described previously (Balbi et al., 1989). In some experiments, digested nuclei were resuspended in a large excess of DM containing 0.5 or 5 mM spermine and, after a 1-h equilibration at 4°C, were collected by centrifugation at 10,000 × *g* and scanned in the buffer supplemented with the polyamine.

RESULTS AND DISCUSSION

Digestion of rat liver chromatin by endogenous nuclease conforms to a random chain-cutting mechanism

The PFGE of DNA isolated from nuclei digested for different times and the corresponding densitometric tracings are reported in Fig. 1. These experiments clearly show the increase in the extent of DNA fragmentation with increasing time of incubation of nuclei in the digestion buffer. However, the electrophoretic patterns of the DNA from different nuclear samples submitted to a 2-h incubation exhibit a somewhat high variability, which can arise from differences both in the initial level of the endogenous nuclease and in the loss of the enzyme occurring during nuclear isolation. This variability is, of course, unimportant for the purpose of this work, which relies on the quantitative (time-independent) correlation between the extent of DNA chain scission and the analysis of the thermal profiles of nuclear chromatin.

On visual inspection of the densitometric tracings it can be immediately concluded that the mode of DNA cleavage by endogenous nuclease does not show any detectable deviation from the behavior expected for a random chain scission process. The curves exhibit only one maximum, which progressively shifts toward lower values of the chain length as the extent of digestion increases. Because we failed to observe digested DNA samples with a biphasic distribution of the lengths of the fragments, we conclude that, at least under our experimental conditions, chromatin superstructure inside the nucleus does not originate from sites with different susceptibilities to the digestion by the nuclease.

The occurrence of a random degradation process can be quantitatively demonstrated by comparing the experimental weight fraction distributions of the chain lengths with the predictions of the theory of random cleavage of long-chain molecules (Montroll and Simha, 1940), using the equation

$$W_t = \frac{\alpha t(1-\alpha)^{(t-1)}}{p+1}[2 + (p - t)\alpha] \qquad (2)$$

where W_t is the weight fraction of the fragment containing t monomeric units connected by $t - 1$ bonds, p is the number of bonds present in the undegraded molecule, and α is the average fraction of cleaved bonds. As we have pointed out in the previous section, it is convenient to express the results in terms of a chain of nucleosomes rather than of DNA; therefore, the monomeric unit and the bond will correspond to the nucleosome and to the linker DNA, re-

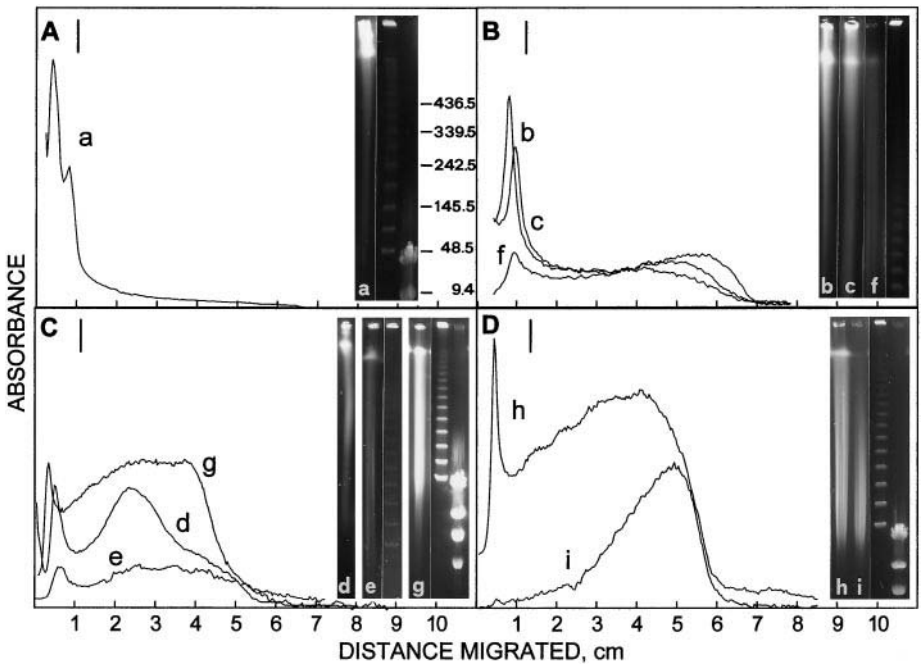

FIGURE 1 Pulsed field gel electrophoretic analysis of the fragmentation of DNA isolated from rat liver nuclei digested for different time periods by activation of endogenous nuclease. The EB stained gels and the corresponding densitometric tracing are marked by the same letter. The incubation times were 0 (*a*), 30 (*b*), 50 (*c*), 75 (*d*), 120 (*e–h*), and 180 min (*i*), respectively. The switch time ramped linearly from 5 to 50 s in the experiments reported in *A*, *C*, and *D*, and from 25 to 75 s in those in *B*. The chain length markers are λ DNA ladder and *Hin*dIII digests of λ DNA; the sizes in kbp are reported on the right of *A*. The peak in the densitometric tracings centered around 1×10^3 kbp corresponds to a spurious band within which long DNA fragments accumulate. The bar corresponds to an absorbance of 0.3 in *A*, 0.15 in *B*, and 0.1 in *C* and *D*.

spectively. Furthermore, p is defined as the average number of linkers present in a chromosome, which can be calculated from the content of genomic DNA and the diploid chromosome number of the cell; for rat hepatocytes we obtain a figure of 7.7×10^5. Equation 2 has been derived for monodisperse samples (all initial molecules have the same molecular weight), while individual chromosomes correspond to DNA stretches of different lengths. The differences in the predicted fragmentation pattern arising from this approximation are small, however, and are very soon lost with increasing α (Balbi et al., 1986).

Because the most probable chain length t_{max} in the distribution curve of the fragments is well approximated by $-1/\log(1 - \alpha)$, provided that p is large (Montroll and Simha, 1940), α can be directly determined from the value of t corresponding to the maximum in the densitometric tracings shown in Fig. 1. The values of α calculated by this method are reported in the left-hand column of the inset in Fig. 2, except for those relative to very mildly digested samples (*tracings b* and *c*), for which t_{max} is too large to be separated electrophoretically. A more accurate value of α can then be obtained by finding the best fit of the weight fraction values to Eq. 2. When the extent of digestion is low, however (*densitometric tracings b* and *c* in Fig. 1), an appreciable amount of DNA (corresponding to 22% and 12% of the weight submitted to electrophoresis, respectively) remains close to the top of the gel, forming a spurious band at $\sim 1 \times 10^3$ kbp, within which fragments of high size accumulate. This effect, which has already been described by another group (Lagarkova et al., 1995), complicates somewhat the calculation of α, because the summation over t in Eq. 1 cannot be accurately evaluated. In this case, it is convenient to eliminate this constant by comparing the experimental ratios of the densitometric areas A_j/A_k with the corresponding theoretical values W_j/W_k; the best value of α representing the data can then been used to calculate the ratios A_j/W_j and hence the average value of $\Sigma A_t \Delta t$. The best fits of the distribution curves to Eq. 2 are shown in Fig. 2, together with the corresponding values of α (*right-hand column in the inset*). The predictions of the random chain scission model are in quantitative agreement with the experiments. Furthermore, the values of α calculated by the best-fit method are very close to the estimates obtained by taking into consideration the most probable chain length (*left-hand column*), in further confirmation of the consistency of the present analysis.

The dimensions of the loop are comparable to the critical size for heterochromatin stability

Early work carried out by DSC in our (Nicolini et al., 1983; Balbi et al., 1989) and in another (Touchette and Cole, 1985) laboratory has shown that micrococcal nuclease digestion of nuclei results in a decrease in the absolute value of the enthalpy of the major endotherm at 106°C, suggesting that the latter is related to the stability of the higher order structure. Subsequent quantitative studies (Cavazza et al., 1991; Barboro et al., 1993; Russo et al., 1995; Labarbe et al., 1996) have confirmed this hypothesis, showing that the thermal transition arises from the denaturation of the DNA of core particles packaged inside ordered (heterochromatic) domains. As we have pointed out previously, this endotherm can be further deconvolved into two component transitions at 100°C and 106°C, the structural origin of which remains to be ascertained, although we tentatively attributed the latter, by inference, to the denaturation of a more stable state arising from the further folding of the 30-nm fiber (Cavazza et al., 1991; Barboro et al., 1993). Biological structures that undergo cooperative unfolding must surpass a critical size to be stable, and therefore the determination of the length of the polynucleosomal chain below which the

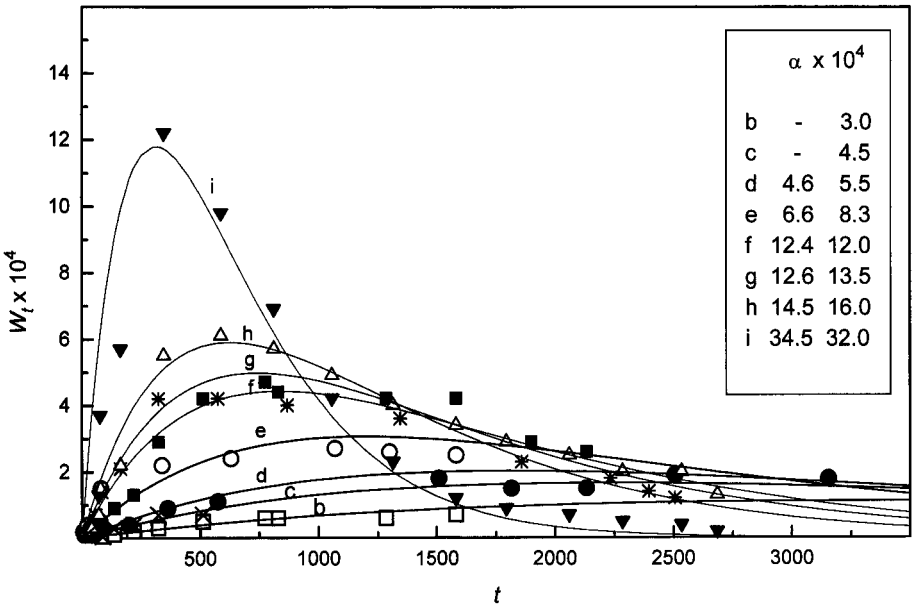

FIGURE 2 Comparison of the experimental weight-fraction chain-length distribution of the DNA isolated from autodigested rat liver nuclei, with the theoretical dependence of W_t on t for a random chain scission process. The distribution curves have been calculated from the electrophoretic experiments reported in Fig. 1; the densitometric tracings and the corresponding distributions are marked by the same letter. The inset reports the values of α calculated from the most probable chain length, corresponding to the maximum in the densitometric tracings (*left-hand column*) and by finding the best fit of the experimental data to the theoretical dependence (*right-hand column*).

106°C endotherm disappears can provide basic conformational information. In our hands, however, digestion experiments of rat liver nuclei with micrococcal nuclease only indicated that the higher order structure is completely lost when the chain length of the DNA drops to a few kbp (Balbi et al., 1989), while we were unable to control the kinetics of digestion at very low enzyme/DNA ratios. This experimental difficulty can be circumvented by using the slow activation of the endogenous nuclease; the results are reported in Fig. 3. The excess heat capacity curves have been deconvolved into Gaussian components, as already described (Cavazza et al., 1991); the major endotherms at 75, 90, 100, and 106°C are marked by III, IV, V_b, and V_a, respectively. Furthermore, it has to be recalled that the low-temperature endotherms between 40°C and 70°C arise from the denaturation of residual (and variable) amounts of cytoskeletal proteins and of the nuclear matrix (Balbi et al., 1989) and, in part, overlap with the melting of the linker DNA (endotherm III), affecting the accuracy of the determination of ΔH_m^{III}. The value of this transition enthalpy is unimportant for the purpose of the present discussion, however. Proteolysis of both H1 and core histones during the isolation of nuclei results in the loss of endotherm V. Although we noticed that the activation of proteases can lead to serious artifacts in the case of calf thymocytes, while rat liver nuclei stored for several days in DM undergo only a limited drift in the thermal profile (Balbi et al., 1989; Russo et al., 1995), the histone complement of both native and digested nuclei has been routinely characterized by sodium dodecyl sulfate-polyacrylamide gel electrophoresis. The insets in Fig. 3, *A*, *C*, *F*, and *H*, show that no proteolytic effect is detectable, even after a prolonged (3 h) incubation in the digestion buffer.

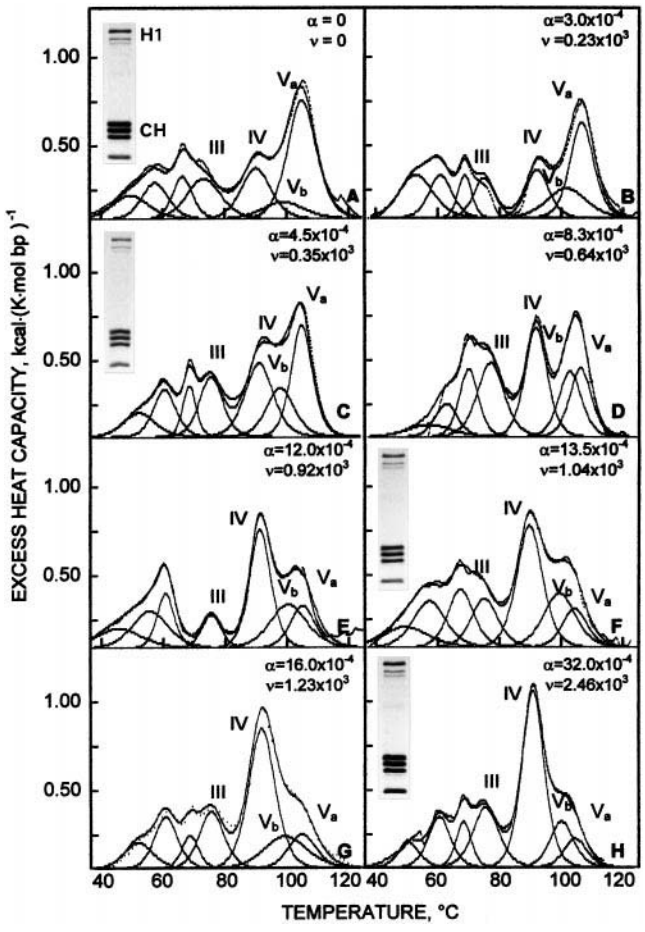

FIGURE 3 Limited DNA digestion by endogenous nuclease induces dramatic structural changes in rat hepatocyte chromatin in situ. For the purpose of a direct comparison with the results reported in the inset of Fig. 2, the extent of double-strand cleavage is expressed in terms of both α and ν. The variability in the low-temperature region of the thermograms reflects differences in the amount of cytoskeletal proteins coisolated with the nuclei. The insets report the electrophoretic characterization of the histone complement isolated from control (*A*) and digested (*C*, *F*, and *H*) nuclei. Histones are designated by H1 and CH (core histones).

For a more direct appreciation of the results, it is convenient to relate the transition enthalpies ΔH_m to ν, the average number of double-strand breaks per chromosome, given by αp. It is apparent that ΔH_m^{Va} dramatically decreases between $\nu = 0$ (Fig. 3 *A*) and $\nu = 0.92 \times 10^3$ (Fig. 3 *E*). The enthalpy loss is almost completely recovered in transition IV, except for a small increase in the heat absorbed in endotherm V_b. This is a well-characterized thermal response, which is observed whenever the higher order structure unfolds; the opposite effect occurs in the course of condensation (Balbi et al., 1989; Cavazza et al., 1991; Barboro et al., 1993; Labarbe et al., 1996). Because transitions IV, V_b, and V_a arise from the denaturation of core particles populating different conformational states, the fractions of core particles f_{IV}, f_{Vb}, and f_{Va} existing in states IV, V_b, and V_a can be obtained by dividing the corresponding transition enthalpies by the total enthalpy change ($\Delta H_m^{IV} + \Delta H_m^{Vb} + \Delta H_m^{Va}$) (Cavazza et al., 1991; Barboro et al., 1993; Russo et al., 1995; Labarbe et al., 1996). The dependence of the fractions defined above on ν is reported in Fig. 4. In line with previous observations on the salt-induced conformational changes (Cavazza et al., 1991), the "more compact" structure corresponding to endotherm V_a

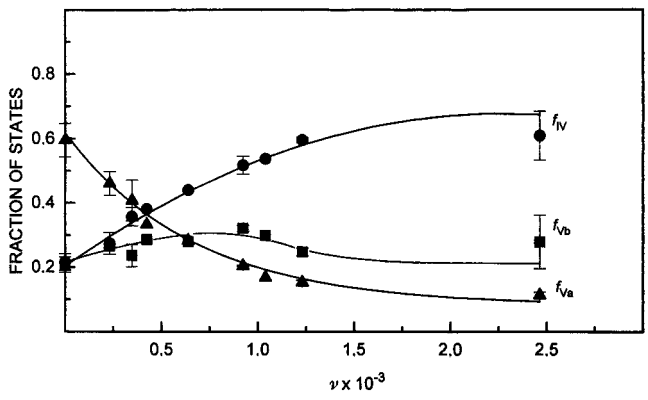

FIGURE 4 Experimental dependence of the fraction of nucleosomes that denature in transitions IV, V_b, V_a on ν, the number of double-strand breaks per chromosome. The bars represent the SD of the mean of four to nine calorimetric determinations.

converts into the "looser" form denaturing in transition V_b, as judged from the small but significant increase in the value of f_{Vb} up to $\nu = 0.75 \times 10^3$. In turn, the latter form unfolds upon limited digestion, giving rise to a large increase in f_{IV}. The consideration of the trends of the fractions of states on ν is sufficient to conclude that the structural change has almost gone to completion for $\nu \cong 2.5 \times 10^3$, a figure that is consistent with the expected number of loops per chromosome, which can be either 4.4 or 1.9×10^3, according to two different estimates of the loop size in rat liver (80 and 35 kbp, respectively) (Igo-Kemenes and Zachau, 1977; Berezney and Buchholtz, 1981). Thus loop and structural target in interphase chromatin have comparable sizes.

The loop behaves like an independent folding unit in heterochromatin formation

We can now attempt to develop a quantitative interpretation of the dependence of f_{Va} on ν by using simple statistical considerations. For this purpose, it is convenient to convert f_{Va} to f_H, the fraction of heterochromatin in digested nuclei normalized for the value in the control (0.6) (Russo et al., 1995). In the case of loops of equal size containing L nucleosomes, the average number of double-strand breaks per loop will be given by $\alpha(L - 1)$. If we assume that one double-strand break per loop is sufficient to unfold the higher order structure locally (within the loop), the value of f_H should be given by the fraction of unbroken loops, which is obtained by Poisson's expression,

$$P_k[\alpha(L-1)] = \frac{[\alpha(L-1)]^k e^{-\alpha(L-1)}}{k!} \qquad (3)$$

where $P_k[\alpha(L - 1)]$ is the probability that a loop receives 0, 1, . . . , k double-strand breaks. In Fig. 5 we compare the experimental dependence of f_H on ν with the values of $P_0[\alpha(L - 1)]$ calculated for L equal to 0.175, 0.40, and 1.0×10^3 nucleosomes, respectively; the first and second values correspond to the two different estimates of the average size of the loop in rat liver nuclei, to which reference has already been made (Berezney and Buchholtz, 1981; Igo-Kemenes and Zachau, 1977). A good agreement with the experiments is observed for $L = 1 \times 10^3$ up to $\nu \cong 1 \times 10^3$; beyond this value the theoretical curve decreases more rapidly than the experimental data. A more adequate treatment, however, must take into account the effect of the size distribution of the loops (van Holde, 1989). The steep decrease of f_H for small values of ν can essentially reflect the unfolding of the loops having a size much larger than the mean, which is due both to the higher probability of receiving a double-strand break and to the larger contribution to f_H compared with loops of smaller size. The dotted curve in Fig. 5, which has been calculated for a distribution of loops containing 0.05, 0.3, and 1.1×10^3 nucleosomes, with frequencies equal to 0.4, 0.35, and 0.25, respectively (average size 0.4×10^3 nucleosomes), represents the data over the entire range much better than that calculated for a monodisperse population of loops of size equal to 0.4×10^3.

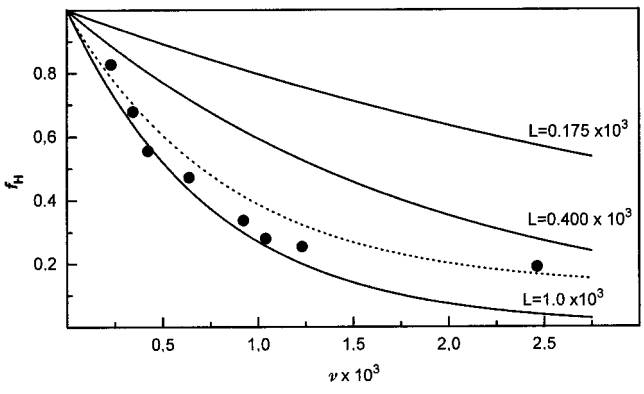

FIGURE 5 Comparison of the experimental dependence of the normalized fraction of heterochromatin f_H with the theoretical fractions of unbroken loops obtained by applying Poisson's distribution. The curves have been calculated for loops containing 0.175, 0.40, and 1.0×10^3 nucleosomes (——) and for a loop size distribution with an average L of 0.40×10^3 (·····).

As a corollary of this analysis, it must be remarked that the decondensation of heterochromatin induced by DNA cleavage conforms to an extremely cooperative (all-or-none) transition mechanism.

Although the use of DSC in combination with the electrophoresis of the DNA represents a self-consistent approach that directly yields the experimental dependence of the average degree of condensation on the fraction of double-strand breaks, it is appropriate to describe briefly the results of preliminary observations in the electron microscope, which have been carried out with the purpose of ascertaining the occurrence of morphological alterations of chromatin in situ relating to the changes in the thermal profile. The nuclei used in the electron microscopy experiments reported in Fig. 6 were collected at different incubation times in the course of the same autodigestion experiment, to circumvent the occurrence of differences in the activity of the endogenous nuclease. The visual inspection of the micrographs gives the impression that the texture of chromatin undergoes a progressive loosening with increasing incubation time. The morphology in the control (Fig. 6, *A* and *B*) appears on the average to be coarser than that found in nuclei isolated after a 3-h incubation (Fig. 6, *G* and *H*), while an intermediate situation is observed after 1 and 2 h (Fig. 6, *C, D* and *E, H*, respectively); no specific structural rearrangement was detected, however. The size distribution curves of the chromatin fibers were therefore determined to characterize the morphological changes by an objective procedure. For each nuclear preparation (see Materials and Methods) several ($\sim 10^3$) values of the linear transverse length L and of the free path between fibers P were independently measured within randomly selected areas of the micrographs; the data are reported in the form of frequency distribution histograms in Fig. 7. For a direct appreciation of the time course of the changes in the mor-

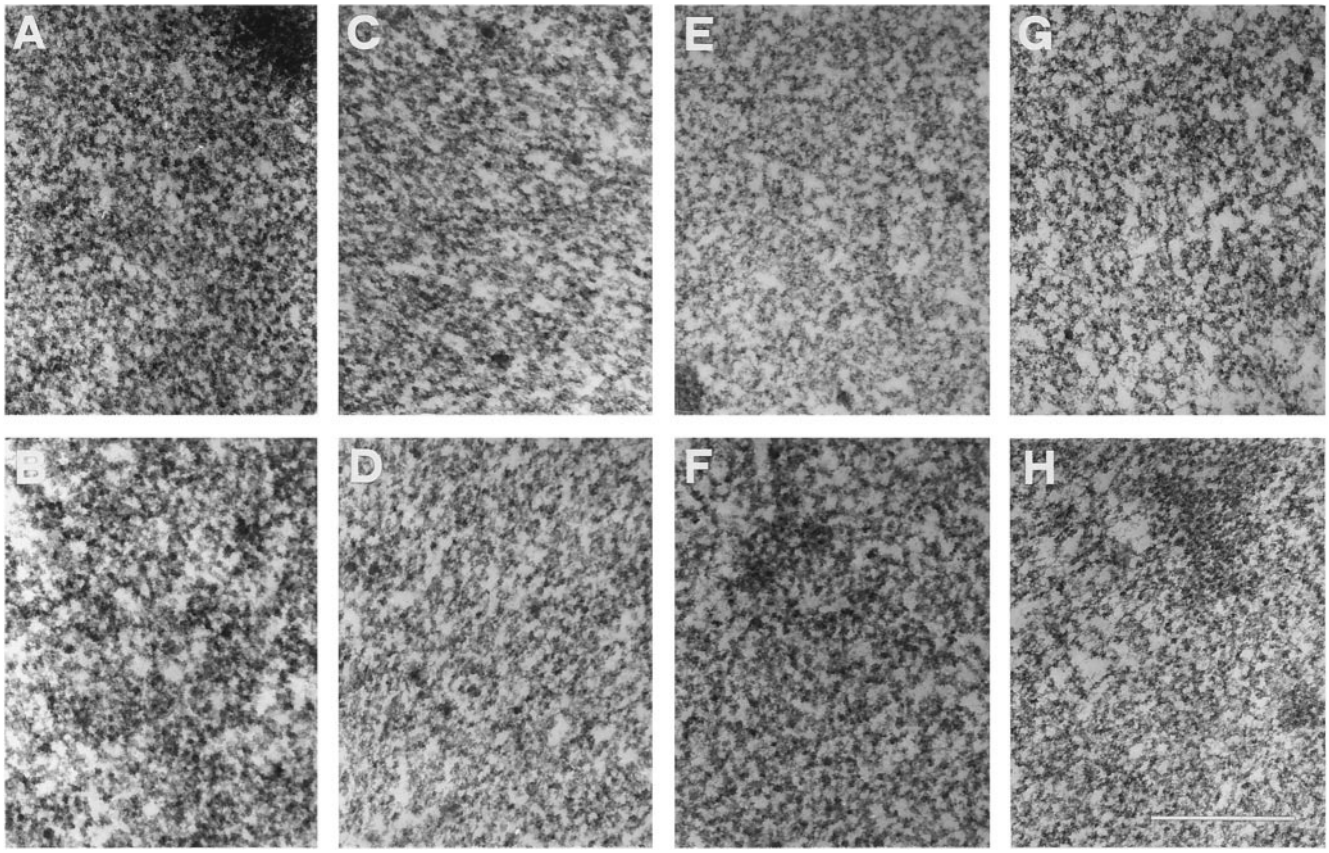

FIGURE 6 Electron micrographs of randomly selected areas of thin sections through rat liver nuclei autodigested for 0 (*A*, *B*), 1 (*C*, *D*), 2 (*E*, *F*), and 3 (*H*, *G*) h. The bar corresponds to 0.5 μm.

phology, the histograms corresponding to 2, 1, and 0 h of incubation were subtracted from those relative to 3, 2, and 1 h, respectively; the difference histograms are reported in the insets of Fig. 7, *B–F*. It has to be noted that the mean linear transverse length across long, randomly oriented rods of radius r corresponds to $2r$ (Fullman, 1953). Because 30-nm fibers as well as their tight aggregates are expected to have cylindrical symmetry, the frequency histograms yield a rough representation of the distribution of the cross-dimensions of the domains of nuclear chromatin; in all of the histograms the mode occurs at 45 nm, a value that is close to the mean linear transverse length of two 30-nm fibers packed side by side.

After 1 h of digestion we observed a decrease in the frequency of large chromatin domains ($L \geq 90$ nm) with respect to control nuclei, while an increase occurs for L between 0 and 60 to 15 nm (*inset* in Fig. 7 *B*); we interpret this effect as the consequence of the partial opening of the larger domains induced by the introduction of a small number of double-strand breaks. The concomitant cleavage of isolated 30-nm fibers cannot be revealed by transverse length measurements, while it is expected to significantly affect the distribution of the free paths. This effect is directly shown in the inset in Fig. 7 *F*, as F increases for large values of P and decreases below 40 nm. After a 2-h digestion this trend reverses. We observe a decrease in F between 0 and 60 nm and an increase beyond 60 nm (*inset* in Fig. 7 *C*), which is correlated with the decrease in the frequency of large free paths (Fig. 7 *G*). We interpret this result as a consequence of the increase in the concentration of chain ends arising from the progressive cleavage of the loop; long chromatin stretches at this point can undergo extensive aggregation, which results both in a limited increase in the transverse length and in a decrease in the free path. This effect becomes more pronounced after 3 h of autodigestion. The frequency histogram of the transverse length undergoes only minor changes with respect to that of nuclei autodigested for 2 h (*inset* in Fig. 7 *D*), while the difference histogram of the free paths shows both a large decrease in the frequency of large P and a concomitant increase around 15 nm. On visual inspection of the electron micrographs reported in Fig. 6, *G* and *H*, it can be concluded that much of the chromatin has the appearance of a closely woven network of knobby fibers.

The effect of spermine on the high-temperature endotherms shows that the folding of nuclear chromatin is a sequential (two-step) process

In our calorimetric method nuclei are, as a rule, isolated and scanned in DM, because a high concentration of EDTA is

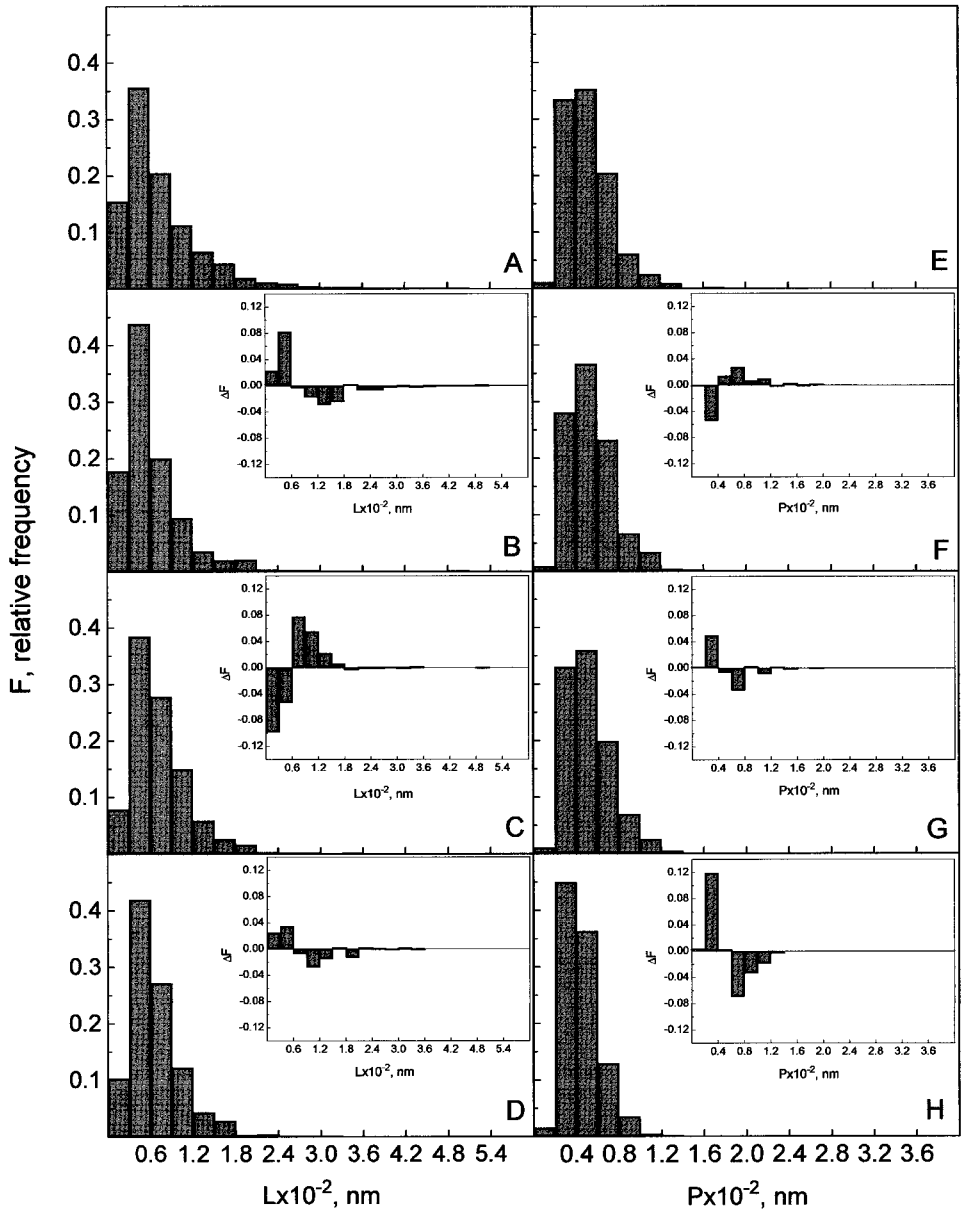

FIGURE 7 Frequency distribution histograms of the linear transverse lengths of the chromatin fibers L (*A–D*) and of the free paths between fibers P (*E–H*), determined from the micrographs of thin sections of rat liver nuclei autodigested for 0 (*A*, *E*), 1 (*B*, *F*), 2 (*C*, *G*), and 3 (*D*, *H*) h. The insets show the difference histograms obtained by subtracting in pairs the distributions of both L and P obtained after 0, 1, and 2 h of digestion from those after 1, 2, and 3 h (*insets* in *B*, *F*, *C*, *G*, *D* and *H*, respectively). The samples were compared using the nonparametric Mann-Whitney U test. The differences between the samples in *F* and *E*, and *G* and *F*, as well as between those in *D* and *C* and those in *B* and *A*, *C* and *B*, and *H* and *G* were found to be significant ($p < 0.04$, $p < 0.0004$, and $p < 0.0001$, respectively).

required to prevent the activation of the Ca^{2+}/Mg^{2+}- or Mg^{2+}-dependent endogenous nucleases (Balbi et al., 1989; Cavazza et al., 1991). Using this buffer, which corresponds to a Na^+ concentration of 0.133 M, we noted that f_{Va}, for nuclei isolated from resting cells, does not appreciably decrease as a consequence of a prolonged incubation in DM (Balbi et al., 1989; Cavazza et al., 1991); condensed chromatin in situ actually does not unfold in the absence of higher valence cations. It could be objected that the apparent stability of the condensed states in native nuclei depends on the slow kinetics of unfolding, rather than on built-in thermodynamic properties. However, we have shown that chromatin can be unfolded and refolded at equilibrium in DM both by changing the ionic strength (Cavazza et al., 1991) and by decreasing or increasing the amount of bound H1 (Russo et al., 1995). Nevertheless, to extrapolate to physiological conditions the results obtained in DM, it is necessary to characterize the unfolding induced by DNA chain scission, also under strong condensation conditions. At physiological concentrations of bivalent cations, short chromatin fragments could undergo the transition to the higher order structure, in contrast to the behavior expected for an all-or-none transition involving the entire loop. Furthermore, the way in which the addition of bivalent or higher valence cations affects the equilibrium values of f_{IV}, f_{Vb}, and f_{Va} can yield information on the overall mechanism of folding.

Both mildly and extensively digested nuclear samples ($\nu = 0.42$ and 1.04×10^3, respectively) were equilibrated with DM containing 0.5 or 5 mM spermine, and the thermal profiles were compared with the results obtained in DM. The latter concentration might be considered exceedingly high, because it has been experimentally observed that in the presence of 5 mM Na^+ the tetravalent cation induces the

condensation of chicken erythrocyte chromatin when its concentration is above 30 μM (Labarbe et al., 1996), in agreement with the predictions of the polyelectrolyte counterion condensation theory. However, by taking into account the results of a careful equilibrium dialysis study (Braunlin et al., 1982), it can be shown that the binding constant of the polyamine to DNA decreases greatly in 0.133 M Na^+ (DM), passing from 6.2×10^4, the value relative to 5 mM Na^+, to 1.32×10^3 M^{-1}. Therefore, at this ionic strength a higher concentration of spermine is required to ensure strong stabilization of the condensed state.

The deconvolved heat capacity curves in Fig. 8 show two important facts. When chromatin has undergone limited digestion ($\nu = 0.42 \times 10^3$) (Fig. 8 *A*), the equilibration of the material with 5 mM spermine sharply increases the enthalpy of transition V_a (Fig. 8 *B*); the experimental values of f_H are equal to 0.56 and 0.80 in DM and in the presence of the polyamine, respectively. By applying Poisson's expression to the loop size distribution of average L equal to 0.4×10^3, as described in the previous section, we find that the increase in the value of f_H (0.24) is comparable with the weight fraction of the loops that have undergone one double-strand break (0.19); in other words, only the loops that have undergone one break are able to undergo refolding. This result confirms that heterochromatin unfolds according to an extremely cooperative mechanism. Second, the increase in f_{Va} apparently occurs at the expense of both f_{IV} and f_{Vb}, which decrease from 0.38 to 0.33 and from 0.29 to 0.20, respectively, a behavior compatible either with the occurrence of two parallel transitions from states IV and V_b or with a sequential mechanism of heterochromatin formation. The latter, however, has been definitively verified by DSC experiments on more extensively digested samples (Fig. 8, *C–E*). At low concentration (Fig. 8 *D*) spermine induces the folding of the unordered state (transition IV) into the intermediate one, as shown by the increase in f_{Vb} from 0.30 to 0.36, while the value of f_{Va} (0.20) increases only slightly, with respect to that of nuclei in the absence of spermine (0.17). With a rise in the concentration of the polyamine to 5 mM (Fig. 8 *E*), however, the value of f_{Vb} (0.31) remains unchanged, within the experimental error, with respect to that determined in DM (0.30), while f_{Va} increases from 0.17 to 0.30. Poisson's analysis of this result indicates again that only the loops that have undergone one double-strand break are able to undergo the transition to heterochromatin; the predicted increase in f_H is 0.30, to be compared with the experimental one (0.22).

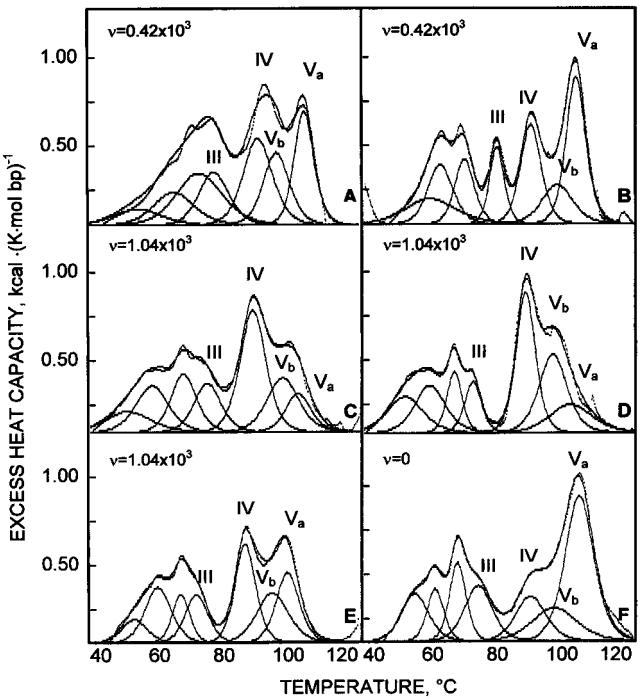

FIGURE 8 Changes in the thermograms of mildly (*A*, *B*) and more extensively (*C*, *D*, and *E*) digested nuclear chromatin induced by the addition of 5 mM (*B*, *E*) and 0.5 mM (*D*) spermine, a strong condensation agent. The results confirm the extremely cooperative nature of transition from state V_b to state V_a (heterochromatin formation) and show that condensation is a sequential (two-step) process. The thermal profile of the nuclear preparation used in the experiments shown in *C, D*, and *E* before digestion is reported for comparison in *F*.

Relation of the present observations on the thermodynamics of chromatin folding to recent concepts of higher order structure

While it is apparent that DSC methods have an extraordinary potential in distinguishing between condensed and unfolded chromatin states (Barboro et al., 1993), it must also be stressed that no thermodynamic approach can directly yield structural information. The problem of the structural attribution of the thermal transitions in the denaturation profiles of proteins and nucleic acids is a central one in biocalorimetry; for example, the attribution of endotherm IV to the melting of DNA in noninteracting core particles relied on the careful comparison of the thermal profile with the temperature dependence of the IR spectrum of unfolded chromatin (Cavazza et al., 1991). Likewise, the increase in the transition enthalpy of endotherm IV at the expense of that of endotherm V, which is the major thermal effect associated with decondensation, was elucidated by monitoring the denaturation profile of chromatin under different salt conditions or by determining the effects of ethidium intercalation and micrococcal nuclease digestion (Balbi et al., 1988, 1989).

The experiments reported in this work show that condensation is a sequential process, involving the all-or-none compaction of the chromatin fiber into higher order structural domains with dimensions comparable to those of the interphase loop. Therefore, one might be tempted to speculate on the possible implications of this new information for the thermodynamic description of permanent gene repression. Knowledge of the major structural features of the nucleosome has recently made possible the quantitative modeling of the dynamics and function of nucleosomal

DNA (Widom, 1998). Unfortunately, the situation is very different as far as the higher order structure is concerned. Both the structure of the 30-nm fiber and the higher levels of compaction lack a definitive experimental demonstration, and, moreover, the basic mechanism of folding of the polynucleosomal chain is being debated (Zlatanova et al., 1998). We shall therefore limit our discussion, without apologies for any particular structural model, the outcomes of our study in relation to the possible molecular determinants of the stability of the 30-nm fiber and of its higher order coiling, which have been closely examined in a recent review (Widom, 1998).

Widom's paper on the physical chemistry of folding of long chromatin fragments (Widom, 1986) reports an exhaustive morphological and structural characterization of the chromatin fiber over a wide concentration range of cations of different valence. The salt-induced refolding of the 11-nm filament into the 30-nm fiber has no end point. The bands at 5.7 and 11 nm in the low-angle x-ray patterns, which have been attributed to the nucleosomal packing in the solenoid, continue to sharpen as the concentration of the mono- or bivalent cation is increased. Widom has pointed out that this effect could depend either on a continuing variation of the helical parameters or on the fluctuation of the polynucleosomal chain between two limit conformational states. As concerns the higher order folding, thick, rope-like aggregates were observed in the electron microscope at high concentrations of Mg^{2+} (from 0.1 to 2 mM, depending on the concentration of Na^{+}). The appearance of the aggregates suggests that the fibers are tightly aggregated and may be interpenetrated.

If one assumes that long chromatin fragments from different sources are in the same conformation under equivalent salt conditions, then our results can be related to Widom's physicochemical model of chromatin folding. Under strong condensation conditions the state giving rise to endotherm V_a is stabilized, a behavior that suggests a relationship of the former to the very tight aggregates of 30-nm filaments, which are the stable state of long chromatin fragments in region III of Widom's phase diagram. Furthermore, because heterochromatin formation is a sequential process that involves the further compaction of the form that denatures in transition V_b, we can also reason that loosely aggregated 30-nm fibers melt in the latter. This comparison suggests that further thermodynamic studies by DSC may be valuable for the purpose of clarifying controversial aspects of the folding of the "unordered" polynucleosomal chain into the 30-nm fiber. Evidence favoring the contention that the 30-nm fiber is a dynamic, marginally stable structure under physiological conditions has recently been reviewed (Widom, 1998). This conclusion is also supported by a previous estimate of the interaction free energy among nucleosomes in the higher order structure ($\Delta G^{int} \cong -5$ kcal per nucleosome mole) obtained in our laboratory (Russo et al., 1995). To fully characterize the transition between the unfolded and helical states, the cooperativity of the process must also be estimated. In our previous DSC study on the thermodynamics of chromatin reconstitution (Russo et al., 1995) we were able to rule out the involvement of a highly cooperative transition mechanism. More stringent experiments are necessary, however, to address the statistical thermodynamics of the conformational change. As we have shown in the previous section, spermine is able to induce, in the case of more extensively digested nuclei, the selective refolding of the "unordered" chain into the state that denatures in transition V_b without appreciable interference of the second condensation step. It is therefore possible to further characterize the folding process as a function of the chain length of the chromatin fragments, an absolute approach that allows the direct determination of both the condensation free energy and the sharpness of the transition.

It has been remarked that the low structural stability of the 30-nm fiber allows the coupling of the binding of transcription factors with chromatin folding (Widom, 1998). This concept can be extended to explain the role of heterochromatin formation in permanent gene repression; the structural stabilization arising from the further coiling of the fiber within the loop might prevent large fluctuations in the local conformation and therefore oppose the binding of transcription factors. Of course, ad hoc models can be envisaged to explain how the proper spatial juxtaposition of the scaffold-associated regions could direct the folding of the 30-nm fiber; for example, a mechanism for chromatin opening has recently been discussed whereby AT-rich sequences at the base of the loop may serve as nucleators of H1 assembly and act as regulators for the H1-induced condensation (Käs et al., 1993).

As we have pointed out above, the development of a quantitative thermodynamic treatment of the higher order folding requires much more detailed structural information than is available at present. A major source of stabilization of heterochromatin is expected to arise, however, from the free energy increase associated with the formation of the loop. Irrespective of the knowledge of the structural parameters, the molecular dynamics simulation, in both the unrestrained and matrix-bound states, of a chain of hard disks connected by flexible segments incorporating the elastic properties of DNA is expected to yield a correct estimate of the free energy of formation of an unfolded chromatin ring anchored to the nuclear scaffold. This study has recently been started in our laboratory.

This work was supported by the Italian Association for Cancer Research (1998), the Ministero della Sanità, and the Ministero dell'Università e della Ricerca Scinetifica e Tecnologica (MURST).

REFERENCES

Allera, C., G. Lazzarini, E. Patrone, I. Alberti, P. Barboro, P. Sanna, A. Melchiori, S. Parodi, and C. Balbi. 1997. The condensation of chromatin in apoptotic thymocytes shows a specific structural change. *J. Biol. Chem.* 272:10817–10822.

Balbi, C., M. L. Abelmoschi, L. Gogioso, S. Parodi, P. Barboro, B. Cavazza, and E. Patrone. 1989. Structural domains and conformational

changes in nuclear chromatin: a quantitative thermodynamic approach by differential scanning calorimetry. *Biochemistry.* 28:3220–3227.

Balbi, C., M. L. Abelmoschi, A. Zunino, C. Cuniberti, B. Cavazza, P. Barboro, and E. Patrone. 1988. The condensation process of nuclear chromatin as investigated by differential scanning calorimetry. *Biochem. Pharmacol.* 37:1815–1816.

Balbi, C., M. Pala, S. Parodi, G. Figari, B. Cavazza, V. Trefiletti, and E. Patrone. 1986. A simple model for DNA elution from filters. *J. Theor. Biol.* 118:183–198.

Barboro, P., I. Alberti, P. Sanna, S. Parodi, C. Balbi, C. Allera, and E. Patrone. 1996. Changes in the cytoskeletal and nuclear matrix proteins in rat hepatocyte neoplastic nodules in their relation to the process of transformation. *Exp. Cell Res.* 225:315–327.

Barboro, P., A. Pasini, S. Parodi, C. Balbi, B. Cavazza, C. Allera, G. Lazzarini, and E. Patrone. 1993. Chromatin changes in cell transformation: progressive unfolding of the higher-order structure during the evolution of rat hepatocytes nodules. A differential scanning calorimetry study. *Biophys. J.* 65:1690–1699.

Berezney, R., and L. A. Buchholtz. 1981. Dynamic association of replicating DNA fragments with the nuclear matrix of regenerating liver. *Exp. Cell Res.* 132:1–13.

Braunlin, W. H., T. J. Strick, and M. T. Record, Jr. 1982. Equilibrium dialysis studies of polyamine binding to DNA. *Biopolymers.* 21: 1301–1314.

Cavazza, B., G. Brizzolara, G. Lazzarini, E. Patrone, M. Piccardo, P. Barboro, S., Parodi, A. Pasini, and C. Balbi. 1991. Thermodynamics of condensation of nuclear chromatin. A differential scanning calorimetry study of the salt-dependent structural transitions. *Biochemistry.* 30: 9060–9072.

Felsenfeld, G. 1996. Chromatin unfolds. *Cell.* 86:13–19.

Filipski, J., J. Leblanc, T. Youdale, M. Sikorska, and P. R. Walker. 1990. Periodicity of DNA folding in higher order chromatin structures. *EMBO J.* 9:1319–1327.

Fullman, R. L. 1953. Measurement of particle sizes in opaque bodies. *Trans. AIME.* 97:447–452.

Igo-Kemenes, T., and H. G. Zachau. 1977. Domains in chromatin structure. *Cold Spring Harb. Symp. Quant. Biol.* 42:109–118.

Käs, E., L. Poljak, Y. Adachi, and U. K. Laemmli. 1993. A model for chromatin opening: stimulation of topoisomerase II and restriction enzyme cleavage of chromatin by distamycin. *EMBO J.* 12:115–126.

Labarbe, R., S. Flock, C. Maus, and C. Houssier. 1996. Polyelectrolyte counterion condensation theory explains differential scanning calorimetry studies of salt-induced condensation of chicken erythrocyte chromatin. *Biochemistry.* 35:3319–3327.

Laemmli, U. K. 1970. Cleavage of structural proteins during the assembly of the head of bacteriophage T4. *Nature.* 227:680–685.

Lagarkova, M. A., O. V. Iarovaia, and S. V. Razin. 1995. Large-scale fragmentation of mammalian DNA in the course of apoptosis proceeds via excision of chromosomal DNA loops and their oligomers. *J. Biol. Chem.* 270:20239–20241.

Montroll, E. W., and R. Simha. 1940. Theory of depolymerization of long chain molecules. *J. Chem. Phys.* 8:721–727.

Nicolini, C., V. Trefiletti, B. Cavazza, C. Cuniberti, E. Patrone, P. Carlo, and G. Brambilla. 1983. Quaternary and quinternary structures of native chromatin and DNA in liver nuclei: differential scanning calorimetry. *Science.* 219:176–178.

Panyim, S., D. Bilek, and R. Chalkey. 1971. An electrophoretic comparison of vertebrate histones. *J. Biol. Chem.* 246:4206–4215.

Parodi, S., F. Kendall, and C. Nicolini. 1975. A clarification of the complex spectrum observed with the ultraviolet circular dichroism of ethidium bromide bound to DNA. *Nucleic Acids Res.* 2:477–486.

Russo, I., P. Barboro, I. Alberti, S. Parodi, C. Balbi, C. Allera, G Lazzarini, and E. Patrone. 1995. Role of H1 in chromatin folding. A thermodynamic study of chromatin reconstitution by differential scanning calorimetry. *Biochemistry.* 34:301–311.

Touchette, N. A., and R. D. Cole. 1985. Differential scanning calorimetry of nuclei reveals the loss of major structural features in chromatin by brief nuclease treatment. *Proc. Natl. Acad. Sci. USA.* 82:2642–2646.

van Holde, K. E. 1989. Chromatin. Springer-Verlag, New York.

Widom, J. 1986. Physicochemical studies of the folding of the 100 Å nucleosome filament into the 300 Å filament. *J. Mol. Biol.* 190: 411–424.

Widom, J. 1998. Structure, dymamics, and function of chromatin in vitro. *Annu. Rev. Biophys. Biomol. Struct.* 27:285–327.

Woodcock, C. L. 1992. The organization of chromosomes and chromatin. *In* Electron Tomography. Three-Dimensional Imaging with the Transmission Electron Microscope. J. Frank, editor. Plenum Press, New York and London. 313–357.

Zlatanova, J., S. H. Leuba, and K. van Holde. 1998. Chromatin fiber structure: morphology, molecular determinants, structural transitions. *Biophys. J.* 74:2554–2566.